Variable-Range Projection Model for Turbulence-Driven Collisions

K. Gustavsson,[1] B. Mehlig,[1] M. Wilkinson,[2] and V. Uski[2]

[1]*Department of Physics, Göteborg University, 41296 Gothenburg, Sweden*

[2]*Department of Mathematics and Statistics, The Open University, Walton Hall, Milton Keynes, MK7 6AA, United Kingdom*

(Received 20 February 2008; published 24 October 2008)

We discuss the relative speeds ΔV of inertial particles suspended in a highly turbulent gas when the Stokes number, a dimensionless measure of their inertia, is large. We identify a mechanism giving rise to the distribution $P(\Delta V) \sim \exp(-C|\Delta V|^{4/3})$ (for some constant C). Our conclusions are supported by numerical simulations, and by the analytical solution of a model equation of motion. The results determine the rate of collisions between suspended particles. They are relevant to the hypothesized mechanism for formation of planets by aggregation of dust particles in circumstellar nebula.

DOI: 10.1103/PhysRevLett.101.174503 PACS numbers: 47.27.−i, 05.40.−a, 45.50.Tn, 92.60.Mt

Introduction.—It is widely believed that the first stage of the formation of planets involves the aggregation of microscopic dust grains in circumstellar accretion disks around young stars [1]. This process must occur in a highly turbulent environment (because the transport of angular momentum by diffusion would be too slow to account for the lifetimes of these disks). The aggregation process occurs in gas with a very low density, so that the motion of the dust grains is very lightly damped. It is necessary to achieve a good understanding of the relative velocity of collisions of the dust grains to determine whether and how planet formation could result from the aggregation of microscopic dust grains. The relative velocity is required to determine the rate of collision of the dust grains. Also, if the relative velocity is sufficiently high, clusters may fragment upon collision. These issues concerning planet formation are discussed in [2,3].

The gas in the circumstellar disk is weakly ionized and behaves as a conventional fluid (rather than a plasma). It exhibits fluctuations characteristic of fluids driven at high Reynolds number ("fully developed turbulence"), which are described by Kolmogorov's statistical theory of turbulence [4]. According to this approach, at lengths well below the driving length scale, fully developed turbulence is a universal phenomenon parametrized by the dissipation rate per unit mass $\mathcal{E}$ and the kinematic viscosity ν.

Earlier discussions of the relative velocity of suspended particles [5–7] have estimated the order of magnitude of the relative velocity, but a satisfactory theory for its distribution has been lacking. In the context of planet formation, the case of lightly damped particles is most important. If the microscopic correlation time of the flow is τ and the damping rate [defined by (2) below] is γ, we define the Stokes number as $\mathrm{St} = 1/\gamma\tau$. A theoretical approach is required, because simulations are impracticable for the lightly damped case where $\mathrm{St} \gg 1$.

In this Letter we show that when $\mathrm{St} \gg 1$ the probability distribution function for the relative velocities ΔV of colliding particles is well approximated by

$$P(\Delta V) = A \exp(-\mathcal{C}|\Delta V|^{4/3}\gamma^{2/3}/\mathcal{E}^{2/3}), \tag{1}$$

where $\mathcal{C}$ is a dimensionless constant (with A determined by normalizing the distribution). We argue that this is a precise asymptote for the distribution for large $|\Delta V|$.

We remark that there are connections with the distribution of accelerations in turbulent flows. The acceleration of a suspended particle is proportional to its velocity relative to the fluid. Because the relative velocity of two particles with $\mathrm{St} \gg 1$ is the sum of their (statistically independent) velocities relative to the fluid, the tail of the distribution of accelerations a of suspended particles is of the form $P(a) \sim \exp[-\mathrm{const}|a|^{4/3}]$, analogous to (1). For suspended particles with $\mathrm{St} \ll 1$, the acceleration is the same as Lagrangian fluid acceleration, which also has a distribution of the same form as (1), with $4/3$ replaced by $\approx 2/5$ [8]. The distribution of accelerations for suspended particles in a turbulent flow was studied numerically for a range of values of St by Bec *et al.* [9]. The results [Fig. 2(b) of their paper] are compatible with the limiting cases discussed above.

Our explanation of the mechanism underlying Eq. (1) proceeds as follows. The colliding particles acquire a relative velocity when they are accelerated by different regions of the fluid. They are then "projected" (i.e., thrown) a certain distance away from the fluid element which accelerated them. Since relative particle velocities imparted by the fluid flow increase with separation, particles which collide with a high relative velocity acquired their relative motion when their separation was large. Our estimate of the probability distribution function $P(\Delta V)$ involves a maximization of the probability of reaching zero separation with respect to variation of the distance over which the particles are projected by the flow. We term this the "variable-range projection" model. It has much in common with the "variable-range hopping" model for electrical conduction in semiconductors at low temperatures [10], which also arises from an optimization of the hopping length and leads to an expression for the conductance of the form (1), with temperature playing the role of the relative velocity.

Our heuristic description is supported by precise asymptotic analysis of a one-dimensional model, Eq. (6) below. Figure 2(a) shows a comparison with results of computer simulations. For nonzero separation, the relative velocity distribution has a more complex asymmetric form, Fig. 2(b). We also confirm a surmise about the variance of the relative velocity of colliding particles [7].

Equations of motion.—The position $\boldsymbol{r}$ and velocity $\boldsymbol{v}$ of a suspended particle obey $\dot{\boldsymbol{r}} = \boldsymbol{v}$ and $\dot{\boldsymbol{v}} = \gamma[\boldsymbol{u}(\boldsymbol{r}, t) - \boldsymbol{v}]$, where $\boldsymbol{u}(\boldsymbol{r}, t)$ is the fluid velocity. This equation is applicable even when the gas mean free path is large compared to the size of the particles [11]. The corresponding equation for the relative displacement $\Delta\boldsymbol{X}$ and relative velocity $\Delta\boldsymbol{V}$ of two particles is

$$\Delta\dot{\boldsymbol{X}} = \Delta\boldsymbol{V}, \qquad \Delta\dot{\boldsymbol{V}} = \gamma[\Delta\boldsymbol{u}(\Delta\boldsymbol{X}, t) - \Delta\boldsymbol{V}], \tag{2}$$

where $\Delta\boldsymbol{u} = \boldsymbol{u}(\Delta\boldsymbol{X}, t) - \boldsymbol{u}(0, t)$. According to Kolmogorov's theory of turbulence, there is a range of length scales ℓ for which a component Δu of the relative velocity of fluid elements with separation ℓ is determined only by $\mathcal{E}$. Dimensional arguments [4] imply

$$\langle \Delta u(\ell, t)\Delta u(\ell, 0)\rangle = (\mathcal{E}\ell)^{2/3} f(t\mathcal{E}^{1/3}/\ell^{2/3}) \tag{3}$$

for some function f (angular brackets are used to denote averages throughout this Letter).

Variable-range projection model.—Consider the relative displacement ΔX and speed ΔV of two particles. When ΔX is small, the driving effect of the fluid velocity Δu is negligible, and the damping term is most significant. At greater distances, the relative velocity of the background fluid drives the relative motion of the particles. First let us consider the relative motion in greater detail at small separations, such that we can neglect the effect of the driving term Δu. In this case ΔV decays exponentially in time, so that if two particles collide with relative velocity ΔV at time t, their relative velocity at an earlier time t_0 was $\Delta V_0 = \Delta V \exp[\gamma(t - t_0)]$. Integrating this expression, we find that the relative separation at time t_0 was

$$\Delta X_0(t_0) = \int_t^{t_0} dt' \Delta V e^{\gamma(t-t')} = \frac{\Delta V}{\gamma}(1 - e^{-\gamma(t-t_0)}). \tag{4}$$

Neglecting the fluid velocity, we see that in order for particles to collide with relative velocity ΔV, they must have had a velocity difference ΔV_0 at a larger, and unknown, separation ΔX_0, satisfying $\Delta V_0 = \Delta V - \gamma\Delta X_0$. For large ΔX, Eqs. (2) resemble those of an Ornstein-Uhlenbeck process [12], where the velocity is Gaussian distributed. For sufficiently large ΔX_0, the relative velocity is therefore approximately Gaussian distributed:

$$\rho(\Delta V_0, \Delta X_0) \sim \frac{1}{\sqrt{2\pi\langle\Delta V_0^2\rangle}} \exp\left[-\left(\frac{\Delta V_0^2}{2\langle\Delta V_0^2\rangle}\right)\right]. \tag{5}$$

We use the expectation that for large separations the relative velocity is well approximated by the relative velocity of the fluid elements: according to (3) the correlation time τ_ℓ at separation ℓ scales as $\ell^{2/3}$. When ΔX_0 is large enough so that $\gamma\tau_{\Delta X_0} \gg 1$, particle separations are advected. Equation (3) then implies that $\langle\Delta V_0^2\rangle \sim (\mathcal{E}\Delta X_0)^{2/3}$. To determine where the inbound particle colliding with relative velocity ΔV originated, we therefore find the value of the separation ΔX_0 which maximizes the probability of colliding with relative velocity ΔV; that is, we maximize $\rho(\Delta V - \gamma\Delta X_0, \Delta X_0)$ with respect to ΔX_0. Figure 1 illustrates the trajectories. Let the value for which the maximum obtains be ΔX_0^*. Neglecting the preexponential factor of (5), we find $\Delta X_0^* = -\Delta V/2\gamma$. The distribution of velocities for colliding particles is predicted to be $P(\Delta V) = \rho(\Delta V - \gamma\Delta X_0^*, \Delta X^*)$. Neglecting the preexponential factor, we obtain Eq. (1). For the variance of the relative velocity, it follows that $\langle\Delta V^2\rangle \propto \mathcal{E}/\gamma$. This provides a justification for a result which was previously inferred from the Kolmogorov theory of fully developed turbulence by a dimensional argument [7].

Microscopic model.—The particle dynamics is characterized by two dimensionless variables. The first is the Stokes number, $\mathrm{St} = 1/\gamma\tau$. The second is the Kubo number, $\mathrm{Ku} = u_K\tau/\eta$. Here u_K is a characteristic velocity, and η and τ refer to the relevant correlation length and correlation time of the flow. In a fully developed turbulent flow, these scales are determined by the motion of the smallest eddies: the Kolmogorov length $\eta = (\nu^3/\mathcal{E})^{1/4}$, the Kolmogorov time $\tau = (\nu/\mathcal{E})^{1/2}$, and the corresponding Kolmogorov velocity $u_K \sim \eta/\tau$. The Kubo number in fully developed turbulence is therefore of the order of unity. However in the following we consider a model for a turbulent flow in which $\mathrm{Ku} \ll 1$, corresponding to a very rapidly fluctuating flow field which can be modeled by a Langevin equation.

Consider the equations of motion (2) in one spatial dimension. We convert to dimensionless variables, writing $t' = \gamma t$, $\Delta x = \Delta X/\eta$, $\Delta v = \Delta V/\eta\gamma$. When the velocity field $\Delta\boldsymbol{u}$ is very rapidly fluctuating, we can approximate the equations of motion in dimensionless variables by the

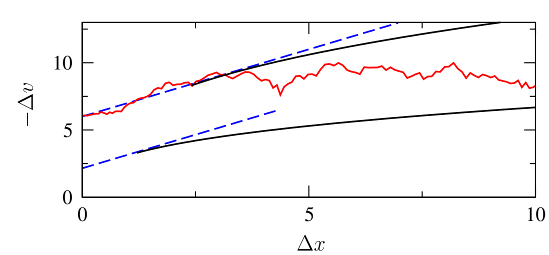

FIG. 1 (color online). Variable-range projection model. We show curves of constant probability $\rho(\Delta x, \Delta v)$ for $\Delta x \gg 1$ (black curve), $\Delta v \propto \Delta x^{1/3}$. Also shown is a realization of a trajectory of Eq. (6) projected from large separations to $\Delta x = 0$ [gray (red) curve], compared with optimal trajectories (blue dashed curve). Here Δx and Δv are dimensionless variables in Eq. (6).

following Langevin equation

$$d\Delta x = \Delta v dt', \qquad d\Delta v = -\Delta v dt' + \delta w, \tag{6}$$

where the random increment δw satisfies

$$\langle \delta w\rangle = 0, \qquad \langle \delta w^2\rangle = 2\mathcal{D}(\Delta x)dt', \qquad \mathcal{D}(\Delta x) = \epsilon|\Delta x|^\alpha. \tag{7}$$

Here we have introduced a parameter ϵ. Having approximated Eqs. (2) by (6), we find that solutions of (6) for different values of ϵ can be obtained from the solution with $\epsilon = 1$ by a scaling transformation. Although it suffices to consider the case where $\epsilon = 1$, we retain ϵ in subsequent expressions because it serves as a small parameter of a WKB expansion. This formal procedure allows us to study the tails of the joint probability distribution of Δx and Δv in a controlled manner. In (7) we also allow for an arbitrary exponent $0 \le \alpha < 2$. The value of α is determined by requiring that $\langle \Delta v^2\rangle$ has the correct behavior as $\Delta x \to \infty$: the solution of (6) presented below suggests that $\langle \Delta v^2\rangle \sim |\Delta x|^\alpha$ for $\Delta x \to \infty$, so comparison with (3) indicates that $\alpha = 2/3$ is the correct choice.

Distribution of collision velocities.—The distribution (1) of collision velocities is determined by the joint distribution $\rho(\Delta x, \Delta v)$ evaluated at $\Delta x = 0$. To determine $\rho(\Delta x, \Delta v)$ we solve the steady-state Fokker-Planck equation corresponding to Eqs. (6) and (7):

$$0 = -\Delta v \partial_{\Delta x}\rho + \partial_{\Delta v}(\Delta v \rho) + \epsilon|\Delta x|^\alpha \partial^2_{\Delta v}\rho. \tag{8}$$

At large values of Δx ($\Delta x \gg \Delta v$), the distribution $\rho(\Delta x, \Delta v)$ is Gaussian in Δv [see Eq. (5)]. In order to solve (8) we make a WKB ansatz [13]

$$\rho(\Delta x, \Delta v) = K(\Delta x, \Delta v)\exp[-S(\Delta x, \Delta v)/\epsilon], \tag{9}$$

$$S(\Delta x, \Delta v) = |\Delta x|^{2-\alpha}\tilde{g}_0(z, \Delta x), \tag{10}$$

$$K(\Delta x, \Delta v) = \exp[-\tilde{g}_1(z, \Delta x)], \tag{11}$$

where $z = s_1\Delta v/\Delta x$ ($s_1 = \pm 1$ is chosen so that $z > 0$). Assuming that $\tilde{g}_0(\Delta x, z)$ does not depend on Δx, substituting (10) and (11) into (8), and collecting terms in ϵ^{-1},

$$g_0'(z) = \frac{1}{2s_1}[z(s_1 + z) + s_2\sqrt{z^2(z + s_1)^2 - 4g_0(z)zs_1(2-\alpha)}], \tag{12}$$

where $s_2 = \pm 1$ labels which branch of the square root is to be chosen. In the following we denote the solutions of (12) by $g_0^{(s_1,s_2)}(z)$. Which of the solutions must be picked is determined by the boundary conditions.

Let us first consider an initial condition $(\Delta x, \Delta v)$ with a positive and large value of Δx. Since $z > 0$ by definition, s_1 determines the sign of Δv. At large values of Δx, the distribution of Δv is Gaussian [Eq. (5)]. This determines the small-z asymptote of g_0: $S = |\Delta x|^{2-\alpha}z^2/2$. Thus we must require $g_0 \sim z^2/2$ as $z \to 0$. We find that only the solutions $g_0^{(-,-)}$ and $g_0^{(+,+)}$ match this boundary condition. In order to reach $\Delta x = 0$ from $\Delta x > 0$, the initial relative velocity must be negative. For $\Delta x > 0$ we are thus forced to choose $s_1 = -1$, that is, to consider the branch $g_0^{(-,-)}$. Consider the case depicted in Fig. 1 of a particle projected to $\Delta x = 0$ determining the distribution of collision velocities. The action is determined by the large-z behavior of $g_0^{(-,-)}$; that is, $S = \lim_{\Delta x\to 0}|\Delta x|^{2-\alpha}g_0^{(-,-)}(-\Delta v/\Delta x)$. We find $g_0^{(-,-)}(z) \sim a_0(\alpha)z^{2-\alpha}$ for large z. The prefactor $a_0(\alpha)$ is determined by numerical integration. We find $a_0(2/3) \approx 0.870$. The resulting action at $\Delta x = 0$ is

$$S(\Delta x = 0, \Delta v) = a_0(\alpha)|\Delta v|^{2-\alpha}. \tag{13}$$

To determine the prefactor, consider terms of order ϵ^0 arising from substituting (10) and (11) into (8):

$$0 = g_0'' - 1 - s_1 xz\partial_x\tilde{g}_1 + (z + s_1z^2 - 2g_0')\partial_z\tilde{g}_1. \tag{14}$$

We make the separation ansatz: $\tilde{g}_1(x, z) = \lambda\log\Delta x + g_1(z)$. It is motivated by the fact that it allows us to match $\rho(\Delta x, \Delta v)$ to the known behavior (5) at large separations. Inserting this ansatz into (14) we obtain (up to a constant)

$$\tilde{g}_1 = \lambda\log\Delta x + \int_{z_0}^{z} dz'\frac{1 - g_0''(z') + s_1\lambda z'}{z' + s_1z'^2 - 2g_0'(z')}. \tag{15}$$

Consider now the limiting form of the prefactor K for large and for small separations Δx. First, the limit of large Δx corresponds to the limit $z \to 0$. In this limit g_1 is constant, and to match the prefactor to the known behavior (5) we must set $\lambda = 3\alpha/2$. Second, the limit of $\Delta x \to 0$ corresponds to the limit of $z \to \infty$. In this limit the integrand in (15) behaves as $\sim\lambda/z' = 3\alpha/(2z')$. Integrating over z we find that $e^{-\tilde{g}_1} = |\Delta v|^{-3\alpha/2}$. The final result (neglecting a normalization factor) is thus

$$\rho(0, \Delta v) = |\Delta v|^{-3\alpha/2}\exp[-\epsilon^{-1}a_0(\alpha)|\Delta v|^{2-\alpha}]. \tag{16}$$

This result, for $\alpha = 2/3$, corresponds to the distribution (1) predicted by the variable-range projection model. But here it has been derived, including the algebraic prefactor, from a microscopic model. Figures 2(a) and 2(c) compare Eq. (16) with computer simulations of the Langevin equations (6) and (7).

Relative velocities at larger separations.—For nonzero separations, our WKB approximation is complicated by the fact that different branches, corresponding to different choices of signs s_1, s_2 in (12), must be combined. For each branch, at finite values of Δx, the contribution to $\rho(\Delta x, \Delta v)$ is of the form (9), with the action given by (10) and (12), and with the prefactor given by Eqs. (11) and (15). Which branches must be chosen depends upon the signs of Δx and Δv. If two branches contribute for given values of Δx and Δv, the branch with the smallest action dominates. The available branches correspond to four different choices of signs in the construction of solutions of (12). We already noted that only the solutions $g_0^{(-,-)}(z)$ and

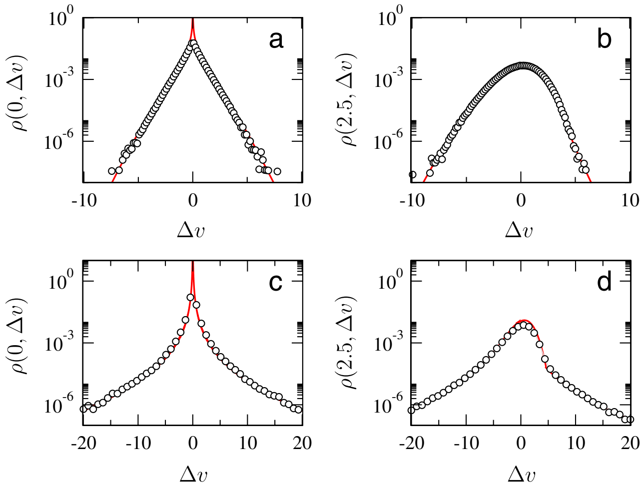

FIG. 2 (color online). Probability density $\rho(\Delta x, \Delta v)$ from computer simulations of Eqs. (6) and (7) (\circ), compared with theory (solid line): (a) $\Delta x = 0$, compared with (1). (b) $\Delta x = 2.5$, compared with (9)–(11). In both cases $\alpha = 2/3$ and $\epsilon = 1$. The numerical results are normalized and the prefactor of the theoretical curves chosen to give the best fit. (c), (d) are the same as for (a) and (b), respectively, except $\alpha = 4/3$.

$g_0^{(+,+)}(z)$ can match the correct asymptotic behavior at small z, namely, $g_0 \sim z^2/2$.

Let us consider the case where $\Delta x > 0$. When $\Delta v < 0$ (that is, when $s_1 = -1$), we find that only the branch with action determined by the function $g_0^{(-,-)}(z)$ contributes, with corresponding action

$$S(\Delta x, \Delta v) = |\Delta x|^{2-\alpha} g_0^{(-,-)}(-\Delta v/\Delta x). \tag{17}$$

This expression tends to (13) as $\Delta v \to -\infty$, and to the Gaussian form $S(\Delta x, \Delta v) \sim \epsilon^{-1}\Delta v^2/|\Delta x|^\alpha$ for small values of Δv.

For $\Delta v > 0$ however, the WKB solution is more complicated. For small z, and for sufficiently small Δv, the solution is given by the branch $g_0^{(+,+)}(z)$. This solution increases very rapidly as z increases, $g_0^{(+,+)}(z) \sim (1 + \alpha)z^3/9$ as $z \to \infty$. So the WKB solution corresponding to this branch becomes very small for large Δv. By adapting the argument above, however, we can argue that the tails of the probability density for the velocity should in fact be given by a branch where the action is $S \sim a_0(\alpha)\Delta v^{2-\alpha}$ for $\Delta v \to \infty$, where the prefactor $a_0(\alpha)$ is the same as for the $\Delta v < 0$ branch. It is possible to find a solution for the branch $g_0^{(+,-)}(z)$ with the correct behavior, namely, $g_0^{(+,-)}(z) \sim a_0(\alpha) z^{2-\alpha}$ as $z \to \infty$. This condition also ensures that the tails of $\rho(\Delta x, \Delta v)$ are consistent with (13) in the limit $\Delta x \to 0$. For $\Delta v > 0$, we therefore construct the solution using two branches. For $0 \le z \le z^*$ the solution obtained from $g_0^{(+,+)}(z)$, satisfying $g_0^{(+,+)}(z) \sim z^2/2$ for $z \to 0$, is dominant. For $z > z^*$, the solution obtained from $g_0^{(+,-)}(z)$, satisfying $g_0^{(+,-)}(z) \sim a_0(\alpha) z^{2-\alpha}$, dominates. The point z^* is determined by the condition that the actions of the two solutions are equal, $g_0^{(+,+)}(z^*) = g_0^{(+,-)}(z^*)$. We remark that the solution $g_0^{(+,-)}(z)$ only exists for $z > z_c$, where z_c is the critical point at which the discriminant in (12) vanishes. Fortunately, we find $z^* > z_c$.

The prefactor is given by Eqs. (11) and (15). Figures 2(b) and 2(d) compare our WKB result for the distribution with those from computer simulations of (6) and (7) for $\Delta x = 2.5$.

Conclusions.—In this Letter we have shown how the distribution of relative velocities of particles suspended in highly turbulent flow at large $\mathrm{St} = 1/(\gamma\tau)$ may be surmised from an optimization argument which we term "variable-range projection," leading to Eq. (1). We validated this simple and general heuristic argument by a WKB analysis of a one-dimensional Langevin model.

We acknowledge discussions with J. Bec and support from Vetenskapsrådet and from the research initiative "Nanoparticles in an interactive environment" at Göteborg University.

[1] P. Goldreich and W.R. Ward, Astrophys. J. **183**, 1051 (1973).
[2] S.V.W. Beckwith, T. Henning, and Y. Nakagawa, in *Protostars and Protoplanets IV*, edited by V. Manning, A.P. Boss, and S. Russell (University of Arizona Press, Tucson, AZ, 2000).
[3] M. Wilkinson, B. Mehlig, and V. Uski, Astrophys. J. Suppl. Ser. **176**, 484 (2008).
[4] U. Frisch, *Turbulence* (Cambridge University Press, Cambridge, England, 1997).
[5] J. Abrahamson, Chem. Eng. Sci. **30**, 1371 (1975).
[6] H.J. Völk, F.C. Jones, G.E. Morfill, and S. Röser, Astron. Astrophys. **85**, 316 (1980).
[7] B. Mehlig, V. Uski, and M. Wilkinson, Phys. Fluids **19**, 098107 (2007).
[8] A. La Porta, G.A. Vith, A.M. Crawford, J. Alexander, and E. Bodenschatz, Nature (London) **409**, 1017 (2001).
[9] J. Bec, L. Biferale, G. Boffetta, A. Celani, M. Cecini, A. Lanotte, S. Musacchio, and F. Toschi, J. Fluid Mech. **550**, 349 (2006).
[10] N.F. Mott, J. Non-Cryst. Solids **1**, 1 (1968).
[11] P.S. Epstein, Phys. Rev. **23**, 710 (1924).
[12] G.E. Ornstein and L.S. Uhlenbeck, Phys. Rev. **36**, 679 (1930).
[13] M.I. Freidlin and A.D. Wentzell, *Random Perturbations of Dynamical Systems* (Springer, New York, 1984).